ACS APPLIED MATERIALS & INTERFACES

Letter

www.acsami.org

Temperature-Dependent Nonlinear Phonon Shifts in a Supported MoS_2 Monolayer

Andrzej Taube,[†] Jarosław Judek, Cezariusz Jastrzębski, Anna Duzynska, Krzysztof Świtkowski, and Mariusz Zdrojek*

Faculty of Physics, Warsaw University of Technology, Koszykowa 75, 00-662 Warsaw, Poland

ABSTRACT: We report Raman spectra measurements on a MoS_2 monolayer supported on SiO_2 as a function of temperature. Unlike in previous studies, the positions of the two main Raman modes, E^1_{2g} and A_{1g} exhibited nonlinear temperature dependence. Temperature dependence of phonon shifts and widths is explained by optical phonon decay process into two acoustic phonons. On the basis of Raman measurements, local temperature change under laser heating power at different global temperatures is derived. Obtained results contribute to our understanding of the thermal properties of two-dimensional atomic crystals and can help to solve the problem of heat dissipation, which is crucial for use in the next generation of nanoelectronic devices.

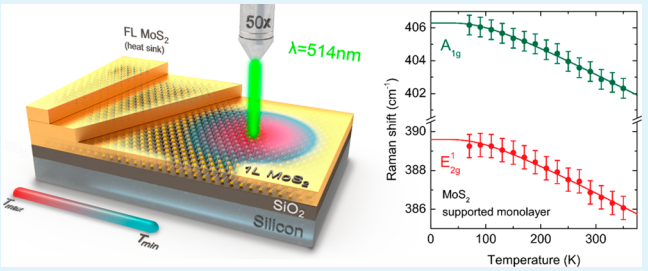

KEYWORDS: *MoS_2 monolayer, two-dimensional atomic crystals, Raman spectroscopy, thermal properties, phonons, laser heating*

Two-dimensional atomic crystals, such as graphene, hexagonal boron nitride, and transition metal dichalcogenides (TMDCs), have attracted considerable attention because of their unique electrical, optical, and mechanical properties.[1−6] The last class of materials is especially interesting for the next generation of electronic and optoelectronic devices because in contrast to graphene, TMDCs are semiconductors with a nonzero bandgap. Among them, molybdenum disulfide, MoS_2, has been the most intensively studied. Its 1.85 eV direct bandgap and presumable high mobility,[7] are properties desirable for the construction of field effect transistors,[8,9] sensors,[10] and photodetectors[11] as well as in the emerging field of valleytronics.[12] Knowledge of a material's thermal properties and a interfacial thermal resistance between adjacent layers[13] is critical for the operation of a variety of electronic devices. This is because heat dissipation is currently one of the most significant constraints on the design and fabrication of integrated electronic circuits. Although MoS_2 has been investigated extensively, there have been few studies[14,15] on its thermal properties, and to the best of our knowledge, none was strictly devoted to supported monolayers of MoS_2. This configuration is important, because it represents the most commonly used device configuration.

In this article, we describe the temperature-dependent nonlinear phonon shifts in supported MoS_2 monolayers. To access the thermal properties of single MoS_2 layers, we used Raman scattering, which is a simple, convenient, and reliable tool used to characterize nanomaterials, such as supported and suspended graphene[16,17] or few-layer MoS_2 flakes at room temperature.[14,15] Especially temperature-dependent Raman shifts can be used to investigate vibration, transport, phonon−phonon properties or electron−phonon interactions.[18] In contrast to previous Raman studies, we show that the positions of the two main Raman modes, E^1_{2g} and A_{1g}, exhibit nonlinear temperature dependence stemming from optical phonon decay. On the basis of obtained results, we calculate how the local temperature of the MoS_2 monolayer changes with different laser power levels.

A schematic of the experimental setup is shown in FIG. 1a, in which a MoS_2 flake placed on the Si/SiO_2 substrate is illuminated by a laser beam focused on a small area on the flake. The laser's role is 2-fold. First, it acts as a source of photons that can be inelastically scattered by phonons in a typical Raman measurement. Second, it serves as a heat source because it can carry a high level of energy that, when absorbed, can significantly increase the local temperature of the sample. Importantly, this temperature increase is reflected in the observed optical phonon energies and lifetimes. Therefore, Raman spectroscopy allows us to increase the local sample temperature and simultaneously yields information about the temperature.

First, the dependence of the phonon energies on temperature is carefully measured. The substrate and the entire MoS_2 flake are the same temperature, and the power of the laser is maintained low enough to not increase the temperature of the irradiated spot. Subsequently, the phonon energy change for the change in laser power level is measured. Combining these measurements, it is possible to determine how the increase of the power level changes the local temperature. We intentionally placed the MoS_2 monolayers on a dielectric substrate because

Received: April 22, 2014
Accepted: June 4, 2014
Published: June 4, 2014

   dx.doi.org/10.1021/am502359k | *ACS Appl. Mater. Interfaces* 2014, 6, 8959−8963

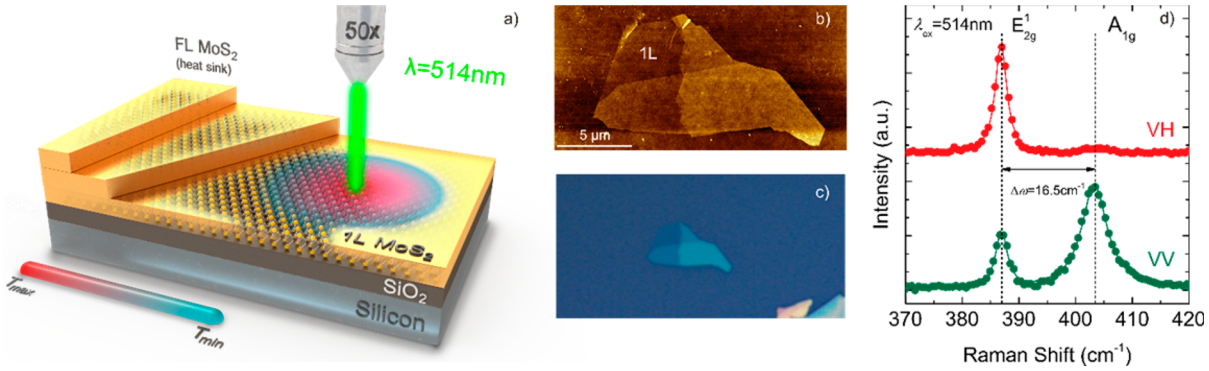

Figure 1. (a) Schematic of the experimental setup; (b) AFM picture of a typical MoS_2 flake and (c) its image from an optical microscope; (d) Raman spectrum of the MoS_2 monolayer at the room temperature and under vacuum for the VV (bottom) and VH (top) light polarization configuration.

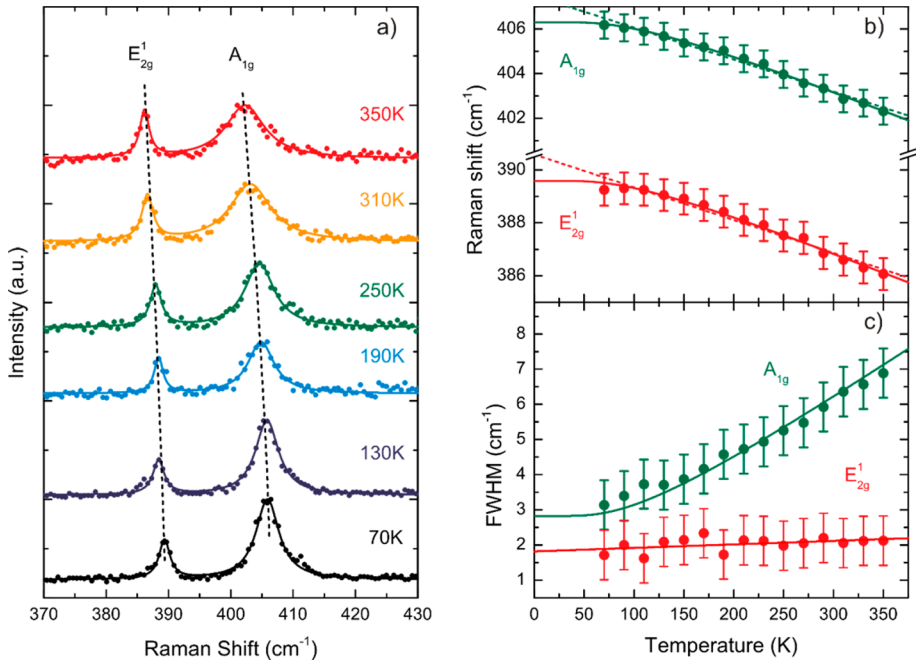

Figure 2. (a) Raman spectra of MoS_2 monolayers measured at selected temperatures from 70 to 350 K. (b) Temperature dependence of the Raman peak positions for the E^1_{2g} and A_{1g} modes. The dashed line represents the fit to eq 2, and the solid line is the fit to eq 3. (c) Measured values of the phonon line widths at temperatures from 70 to 350 K. The solid line for the A_{1g} mode represents the fit from eq 4. The error bars represent the expanded uncertainty at the 95% level of confidence and include finite spectral resolution and the average uncertainty of determination of peak position (~0.1 cm^{-1}) or fwhm (~0.2 cm^{-1}).

thermal properties determined in this way better describe that in real devices.

The MoS_2 flakes were fabricated using conventional mechanical exfoliation from MoS_2 single crystals (SPI) and then transferred to the Si/SiO_2 substrate.[19] Optical microscopy, atomic force microscopy, and Raman spectroscopy were employed to identify the monolayers.[20] FIG. 1b shows a folded flake, with the region denoted as 1L confirmed to be a single layer. The thickness from AFM studies was 0.65−0.7 nm, typical for a MoS_2 monolayer on a SiO_2 substrate.[21] Raman spectra taken by a Dilor XY-800 spectrometer using an Ar laser at 514 nm (2.41 eV) excitation in the VV light polarization configuration (the electric field vectors of the incident light and scattered light are parallel) show two active modes, denoted[22] as E^1_{2g} and A_{1g} (Figure 1d). In the VH light polarization (the electric field vectors of the incident light and scattered light are perpendicular) only E^1_{2g} mode was observed. Therefor VV configuration is more suitable for our experiment. Differences in Raman spectra taken in VV and VH configuration originate in symmetry selection rules.

A single layer of molybdenum disulfide consists of two hexagonal planes of sulfur atoms linked by covalent bonds with the hexagonal plane of molybdenum atoms in the middle. The A_{1g} mode is associated with the out-of-plane vibrations of the sulfur atoms, whereas the E^1_{2g} mode is related to the in-plane vibrations of the sulfur and molybdenum atoms. The difference between the positions of these two modes depends on the number of layers in the flake, and for a monolayer equals 18.5 cm^{-1} under ambient atmosphere[23] and 16.5 cm^{-1} in vacuum. This effect is attributed to environmental effects, particularly to the desorption of various molecules from the MoS_2 surface.[24] Temperature-dependent Raman spectra were obtained while heating and cooling the samples in a microscope cryostat in which the temperature was controlled between 70 and 350 K with a stability of approximately 0.1 K. The laser power on the sample was carefully calibrated and set between 30 and 60 μW.

dx.doi.org/10.1021/am502359k | ACS Appl. Mater. Interfaces 2014, 6, 8959−8963

The results of the temperature-dependent Raman study are presented in Figure 2. In Figure 2a, spectra for selected temperatures from 70 to 350 K are shown to illustrate the Raman spectra evolution. The downshift and broadening of the peaks can be easily observed. However, to perform a more quantitative analysis, we calculated the positions and widths (fwhm) of both observed peaks and plotted them in panels b and c in Figure 2 (see ref 25 for details). Interestingly, at low temperatures, it can be seen a clear deviation from linear temperature dependence of both positions and the line width. We note that subsequent measurements and measurements on different samples not give much difference in obtained results. We remind that the peak position (Raman shift) is attributed to the phonon energy ($\hbar\omega$), whereas the fwhm is related to the phonon lifetime.

Generally, temperature dependence of Raman shifts and line widths arises from electron−phonon, anharmonic phonon−phonon interactions and thermal expansion.[18,26] Particularly, one can use these factors to understand observed temperature dependence of Raman spectra. For example negative temperature dependence of graphene G-mode line width after Ar annealing can be associated with electron−phonon interactions[26] whereas positive temperature dependence of multilayer MoS_2 A_{1g} mode line width can be explained by optical phonon decay.[14] In our case, to describe the phonon softening (decrease in phonon energy) due to the temperature increase, we employed two approaches that have been used in numerous studies. In the first one, a linear change in the energy with temperature is assumed by[17,27]

$$\omega(T) = \omega_0 + \chi T \tag{1}$$

where ω_0 is the phonon frequency at zero temperature and χ is the first-order temperature coefficient. Fitting our results to expression 1, we obtained parameters that were in good agreement with other works (see Table 1 for details). The linear fit to our data is represented by the dashed line in Figure 2b.

Table 1. Temperature Dependence of the Positions of the E^1_{2g} and A_{1g} MoS_2 Modes for Suspended (susp.) or Substrate Supported (sup.) Layers[a]

	χ (cm^{-1}/K)	
	A_{1g}	E^1_{2g}
this work, sup. monolayer, EX	−0.0143	−0.0124
ref 14, susp. multilayer, EX	−0.0123	−0.0132
ref 15, sup. monolayer, EX	−0.013	−0.017
ref 15, susp. monolayer, EX	−0.013	−0.011
ref 27, sup. monolayer, CVD	−0.016	−0.013
ref 27., sup. multilayer, EX	−0.013	−0.015

[a]CVD, chemical vapor deposition; EX, mechanical exfoliation.

The second approach is based on a phenomena of the optical phonon decay of two acoustic phonons with equal energies due to lattice potential anharmonicity. A useful formula was proposed by Balkanski[28]

$$\omega(T) = \omega_0 + A\left(1 + \frac{2}{e^x - 1}\right) \tag{2}$$

where $x = \hbar(\omega_0/2)/k_BT$ and A is an anharmonic constant. The values of the fitting parameters are listed in Table 2. We found that this approach, represented by the solid lines in Figure 2b,

Table 2. Temperature Dependence of the Positions and FWHMs of the E^1_{2g} and A_{1g} Modes[a]

	A_{1g}	E^1_{2g}
ω_0 (cm^{-1})	408.9	391.7
A (cm^{-1})	−2.61	−2.15
Γ (cm^{-1})	29.82	

[a]For the E^1_{2g} mode, the changes in the FWHM are lower than the uncertainties.

was more appropriate for the description of $\omega(T)$ because it better fit the experimental data at low temperatures (<150 K). We note that measurable changes in phonon energies versus temperature are a necessary condition for the applicability of our method. Therefore, in the case of saturation of the phonon energies at low T, it could be impossible to reliably estimate small temperature changes from the peak position changes. Fortunately, this situation does not take place in our study. It is also interesting that such nonlinear behavior, shown here in the case of single-layer MoS_2, was also recently observed for supported WS_2 single layers.[29] However, the authors attributed this nonlinearity to experimental artifacts and used eq 1 to describe the phonon energy shifts with temperature.

For higher temperatures, taking into account only first-order Taylor expansion, the two theoretical curves converge because eq 2 converts to a linear dependence

$$\omega(T) \xrightarrow{x=\hbar\omega_0/2k_BT\ll 1} \omega_0 + A + \frac{4Ak_B}{\hbar\omega_0}T = \omega_0' + \chi_B T,\ \omega_0' = \omega_0 + A,\ \chi_B = \frac{4Ak_B}{\hbar\omega_0}T \tag{3}$$

with slope values of −0.0178 and −0.0152 cm^{-1}/K for the E^1_{2g} and A_{1g} modes, respectively. Differences from the data in Table 1 originate from the smaller number of experimental points in the linear regime.

Figure 2c shows the temperature dependence of the Raman peak widths (fwhm) for both the experimental data and the theoretical curves. It can be seen that the changes in the width of the E^1_{2g} peak are almost negligible. The linear fits are only a guide for the eye. On the contrary, the width of the A_{1g} peak exhibited strong temperature changes. The theoretical dependence of the fwhm of the peak is obtained by the expression[28]

$$\Gamma(T) = \Gamma_0\left(1 + \frac{2}{e^x - 1}\right) \tag{4}$$

where Γ_0 is the peak width at zero temperature. The fit parameter is shown in Table 2 only for the A_{1g} mode because the E^1_{2g} mode does not follow the predictions of this theory. The peak width could also be considered a temperature indicator. Particularly one can use $\Delta\Gamma$ instead of $\Delta\hbar\omega$. In our work, we used a traditional approach because the uncertainties in estimating the temperature from the peak position shifts were lower than those from the peak width.

We have shown the experimental data and theoretical models for both Raman modes. However, for further data processing, as a temperature indicator, the position of the A_{1g} symmetry mode was chosen because of its higher intensity and slightly larger changes with T. For the temperature estimation, we used the dependence determined by fitting with eqs 1 and 2 instead of taking the raw data.

To determine how laser power level changes local MoS_2 temperature, we measured two Raman spectra at every

dx.doi.org/10.1021/am502359k | ACS Appl. Mater. Interfaces 2014, 6, 8959−8963

temperature, one for P_{in} = 30 μW and the second for P_{in} = 60 μW, where P_{in} represents the laser power on the sample. An example result taken for T = 310 K is shown in FIG. 3a. For higher laser powers, the Raman peaks clearly downshift as a result of local heating. The complete set of peak frequency changes is presented in Figure 3b. We note that the dependence of the peak position is not a monotonic function of temperature and has a maximum at T = 150 K. Below this temperature, the heat dissipation process becomes less effective owing to optical phonon decay, as explained above. Calculations for the temperature rise due to the laser power increase were performed in the following way. At a fixed global temperature (temperature of the cryostat and the entire sample without laser illumination), we calculated the temperature corresponding to the A_{1g} mode peak positions for the two laser powers (using the data presented in Figures 2b and 3b). The difference was called the local temperature change and is depicted in Figure 3c. The minimum ΔT increase coincides with the minimal Raman shift from Figure 3b. We note that the local temperature was estimated on the basis of both fitted curves describing the temperature dependence of the Raman peak position for mode A_{1g}. The divergences at low and high temperatures are quite intuitive with respect to Figure 2b and originate in the differences between the assumed models discussed earlier. The minimum of ΔT indicates that the most efficient heat dissipation in supported MoS_2 monolayer occurs at T = 150 K. This knowledge can be used for proper thermal management of nanoscale electrical devices. This is important finding, because in real devices, like graphene transistors on SiO_2/Si substrates, most of the heat power is dissipated by layers lying below conductive channel. Local temperature change at different global temperature and constant heating power might be related to changes in the thermal conductivity[16] or the interfacial thermal resistance.[13] Our results may be further used to determine temperature dependence of above-mentioned quantities.

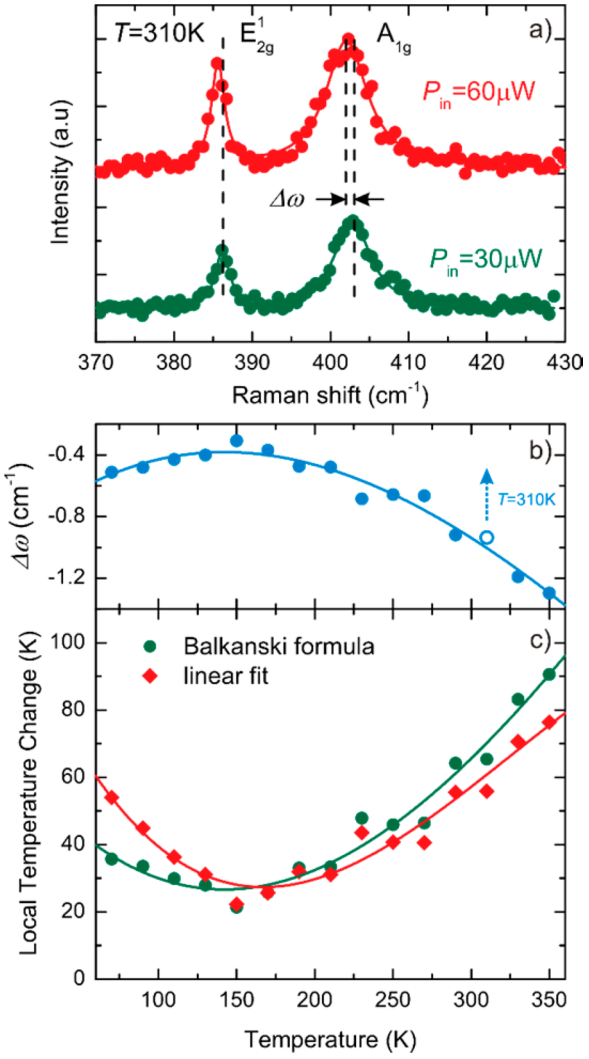

Figure 3. (a) Raman spectra of single layer MoS_2 for different incident laser powers taken at 310 K. (b) Change in the A_{1g} peak position due to the absorbed laser power at different temperatures. (c) Calculated local temperature change. All solid lines are only guides for viewing.

In conclusion, we have experimentally studied the temperature-dependent Raman spectra of a supported MoS_2 monolayers at temperatures between 70 and 350 K. We found that Raman shifts exhibits nonlinear temperature dependence. We conclude that obtained effects stem from the optical phonon decay and lattice potential anharmonicity in the MoS_2 monolayer. In high temperatures, phonon shifts were described by first-order temperature coefficients, which was −0.0178 and −0.0152 cm^{-1}/K for the A_{1g} and E^1_{2g} modes, respectively. On the bassis of Raman measurements, local temperature change of supported MoS_2 monolayer under laser heating power was calculated as a function of different global temperatures. The minimum temperature rise ΔT = 20 was observed at T = 150 K. We claim that observed effect is related to thermal conductivity changes of monolayer MoS_2 and more effort is needed to explain this in details. Our results may be useful for further experimental and theoretical studies on the thermal properties of two-dimensional atomic crystals based on MoS_2 and other dichalcogenides single layers.

AUTHOR INFORMATION

Corresponding Author

*E-mail: zdrojek@if.pw.edu.pl.

Present Address

†A.T. is also with Institute of Electron Technology, Warsaw, Poland and with Institute of Microelectronics and Optoelectronics, Warsaw University of Technology, Warsaw, Poland.

Notes

The authors declare no competing financial interest.

ACKNOWLEDGMENTS

The work was supported by the Polish Ministry of Science and Higher Educationwithin the Diamond Grant programme (0025/DIA/2013/42). A.T. and A.D. were also supported by the European Union in the framework of the European Social Fund through the Warsaw University of Technology Development Programme.

REFERENCES

(1) Novoselov, K. S.; Jiang, Z.; Zhang, Y.; Morozov, S. V.; Stormer, H. L.; Zeitler, U.; Maan, J. C.; Boebinger, G. S.; Kim, P.; Geim, A. K. Room-Temperature Quantum Hall Effect in Graphene. *Science* **2007**, *315*, 1379.

(2) Nair, R. R.; Blake, P.; Grigorenko, A. N.; Novoselov, K. S.; Booth, T. J.; Stauber, T.; Peres, N. M. R.; Geim, A. K. Fine Structure Constant Defines Visual Transparency of Graphene. *Science* **2008**, *320*, 1308.

(3) Wang, Q. H.; Kalantar-Zadeh, K.; Kis, A.; Coleman, J. N.; Strano, M. S. Electronics and Optoelectronics of Two-Dimensional Transition Metal Dichalcogenides. *Nat. Nanotechnol.* **2012**, *7*, 699−712.
(4) Late, D. J.; Liu, B.; Luo, J.; Yan, A.; Ramakrishna Matte, H. S. S.; Grayson, M.; Rao, C. N. R.; Dravid, V. P. GaS and GaSe Ultrathin Layer Transistors. *Adv. Mater.* **2012**, *24*, 3549−3554.
(5) Rout, C. S.; Joshi, P. D.; Kashid, R. V.; Joag, D. S.; More, M. A.; Simbeck, A. J.; Washington, M.; Nayak, S. K.; Late, D. J. Superior Field Emission Properties of Layered WS_2-RGO Nanocomposites. *Sci. Rep.* **2013**, *3*, 3282.
(6) Kashid, R. V.; Late, D. J.; Chou, S. S.; Huang, Y.-K.; De, M.; Joag, D. S.; More, M. A.; Dravid, V. P. Enhanced Field-Emission Behavior of Layered MoS_2 Sheets. *Small* **2013**, *9*, 2730−2734.
(7) Fuhrer, M. S.; Hone, J. Measurement of Mobility in Dual-Gated MoS_2 Transistors. *Nat. Nanotechnol.* **2013**, *8*, 146−147. and B. Radisavljevic, B.; Kis, A. Reply to 'Measurement of Mobility in Dual-Gated MoS_2 Transistors'. *Nat. Nanotechnol.* **2013**, *8*, 147−148.
(8) Late, D. J.; Liu, B.; Ramakrishna Matte, H. S. S.; Dravid, V. P.; Rao, C. N. R. Hysteresis in Single-Layer MoS_2 Field Effect Transistors. *ACS Nano* **2012**, *14*, 5635−5641.
(9) Wang, H.; Yu, L.; Lee, Y. H.; Shi, Y.; Hsu, A.; Chin, M. L.; Li, L. J.; Dubey, M.; Kong, J.; Palacios, T. Integrated Circuits Based on Bilayer MoS_2 Transistors. *Nano Lett.* **2012**, *9*, 4674−4680.
(10) Late, D. J.; Huang, Y.-K.; Liu, B.; Acharya, J.; Shirodkar, N. S.; Luo, J.; Yan, A.; Charles, D.; Waghmare, U. V.; Dravid, V. P.; Rao, C. N. R. Sensing Behavior of Atomically Thin-Layered MoS_2 Transistors. *ACS Nano* **2013**, *7*, 4879−4891.
(11) Lopez-Sanchez, O.; Lembke, D.; Kayci, M.; Radenovic, A.; Kis, A. Ultrasensitive Photodetectors Based on Monolayer MoS_2. *Nat. Nanotechnol.* **2013**, *8*, 497−501.
(12) Mak, K. F.; He, K.; Shan, J.; Heinz, T. F. Control of Valley Polarization in Monolayer MoS_2 by Optical Helicity. *Nat. Nanotechnol.* **2012**, *7*, 494−498.
(13) Freitag, M.; Steiner, M.; Martin, Y.; Perebeinos, V.; Chen, Z.; Tsang, J. C.; Avouris, P. Energy Dissipation in Graphene Field-Effect Transistors. *Nano Lett.* **2009**, *9*, 1883−1888.
(14) Sahoo, S.; Gaur, A. P. S.; Ahmadi, M.; Guinel, M. J.-F.; Katiyar, R. S. Temperature-Dependent Raman Studies and Thermal Conductivity of Few-Layer MoS_2. *J. Phys. Chem. C* **2013**, *117*, 9042−9047.
(15) Yan, R.; Simpson, J. R.; Bertolazzi, S.; Brivio, J.; Watson, M.; Wu, X.; Kis, A.; Luo, T.; Hight Walker, A. R.; Grace Xing, H. Thermal Conductivity of Monolayer Molybdenum Disulfide Obtained from Temperature-Dependent Raman Spectroscopy. *ACS Nano* **2014**, *8*, 986−993.
(16) Cai, W.; Moore, A. L.; Zhu, Y.; Li, X.; Chen, S.; Shi, L.; Ruoff, R. S. Thermal Transport in Suspended and Supported Monolayer Graphene Grown by Chemical Vapor Deposition. *Nano Lett.* **2010**, *10*, 1645−1651.
(17) Balandin, A.; Ghosh, S.; Bao, W.; Calizo, I.; Teweldebrhan, D.; Miao, F.; Lau, C. N. Superior Thermal Conductivity of Single- Layer Graphene. *Nano Lett.* **2008**, *8*, 902−907.
(18) Late, D. J.; Maitra, U.; Panchakarla, L. S.; Waghmare, V. U.; Rao, C. N. R. Temperature Effects on the Raman Spectra of Graphenes: Dependence on the Number of Layers and Doping. *J. Phys.: Condens. Matter* **2011**, *23*, 055303.
(19) Novoselov, K. S.; Jiang, D.; Schedin, F.; Booth, T. J.; Khotkevich, V. V.; Morozov, S. V.; Geim, A. K. Two-Dimensional Atomic Crystals. *Proc. Natl. Acad. Sci. U.S.A.* **2005**, *102*, 10451−10453.
(20) Late, D. J.; Liu, B.; Ramakrishna Matte, H. S. S.; Rao, C. N. R.; Dravid, V. P. Rapid Characterization of Ultrathin Layers of Chalcogenides on SiO_2/Si Substrates. *Adv. Funct. Mater.* **2012**, *22*, 1894−1905.
(21) Radisavljevic, B.; Radenovic, A.; Brivio, J.; Giacometti, V.; Kis, A. Single-Layer MoS_2 Transistors. *Nat. Nanotechnol.* **2011**, *6*, 147−150.
(22) There is a different notation of main Raman modes for different point group of even and odd MoS_2 layers (i.e., S-Mo-S tri layers). The odd numbers of MoS_2 layers with no inversion symmetry belongs to the D_{3h} point group and main Raman modes are noted as E' and A_1'. The even number of MoS_2 layers with inversion symmetry belongs to the D_{6h} and main Raman modes are noted as E^1_{2g} and A_{1g}. See *Phys. Rev. B* **2013**, *87*, 115413 for details. However, in many publications, the main Raman modes of monolayer MoS_2 are noted as E^1_{2g} and A_{1g}.
(23) Lee, C.; Yan, H.; Brus, L. E.; Heinz, T. F.; Hone, J.; Ryu, S. Anomalous Lattice Vibrations of Single- and Few-Layer MoS_2. *ACS Nano* **2010**, *4*, 2695−2700.
(24) Zhang, W.; Huang, J.-K.; Chen, C.-H.; Chang, Y.-H.; Cheng, Y.-J.; Li, L.-J. High-Gain Phototransistors Based on a CVD MoS_2 Monolayer. *Adv. Mater.* **2013**, *25*, 3456−3461.
(25) Two Lorentzian functions (one for E^1_{2g} and one for A_{1g}, respectively) were fitted to the experimental data using the Levenberg−Marquard algorithm. The error bars correspond to the expanded uncertainty at the 95% level of confidence and include the finite spectral resolution and the uncertainty in the determination of the peak position or the fwhm. The extended uncertainty was calculated using the following formula: $u(\omega) = k(S_\omega^2 + (\Delta\omega)^2/3)^{1/2}$, where $k = 2$ for the 95% level of confidence, s_ω stands for the error obtained from the fitting procedure, and $\Delta\omega$ represents the resolution of the spectrometer (0.5 cm^{-1} for measurements in one spectral window).
(26) Abdula, D.; Ozel, T.; Kang, K.; Cahill, D. G.; Shim, M. Environment-Induced Effects on the Temperature Dependence of Raman Spectra of Single-Layer Graphene. *J. Phys. Chem. C* **2008**, *112*, 20131−20134.
(27) Lanzillo, N. A.; Birdwell, A. G.; Amani, M.; Crowne, F. J.; Shah, P. B.; Najmaei, S.; Liu, Z.; Ajayan, P. M.; Lou, J.; Dubey, M.; Nayak, S. K.; O'Regan, T. P. Temperature Dependent Phonon Shifts in Monolayer MoS_2. *Appl. Phys. Lett.* **2013**, *103*, 093102.
(28) Balkanski, M.; Wallis, R. F.; Haro, E. Anharmonic Effects in Light Scattering Due to Optical Phonons in Silicon. *Phys. Rev. B* **1983**, *28*, 1928.
(29) Thripuranthaka, M.; Late, D. J. Temperature Dependent Phonon Shifts in Single-Layer WS_2. *ACS Appl. Mater. Interfaces* **2014**, *6*, 1158−1163.